Macromolecules
ARTICLE

Macromolecules **2009**, *42*, 8477–8484 **8477**
DOI: 10.1021/ma9016339

Vesicle Formation of PLA_x-PEG_{44} Diblock Copolymers

Binyang Du,*,† Aixiong Mei,† Kezheng Yin,† Qinfen Zhang,‡ Junting Xu,† and Zhiqiang Fan†

†*Key Laboratory of Macromolecular Synthesis and Functionalization* (*Ministry of Education*), *Department of Polymer Science & Engineering, Zhejiang University, Hangzhou 310027, China, and* ‡*BioEM lab, State Key Lab of Biocontrol, School of life Sciences, Sun Yat-Sen University, Guangzhou 510275, China*

Received July 23, 2009; Revised Manuscript Received October 6, 2009

ABSTRACT: Three PLA_x-PEG_{44} diblock copolymers with fixed hydrophilic PEG block and various lengths of hydrophobic PLA block were synthesized via ring-opening polymerization. The micelle formation and micelle morphologies of the PLA_x-PEG_{44} copolymers in selective solvents were investigated by using cryogenic transmission electron microscopy (cryo-TEM) and light scattering techniques. PLA_x-PEG_{44} diblock copolymers in aqueous solution form various micelle structures when increasing x from 56 to 212 in order to minimize the overall free energy of the systems. The micelles transform from wormlike micelles for $PLA_{56}-PEG_{44}$ into vesicles for $PLA_{212}-PEG_{44}$. Interestingly, vesicular structures with various morphologies, such as large polydisperse vesicles, entrapped vesicles, hollow concentric vesicles, ellipsoidal vesicles, open bending lamellae, vesicles with irregular shapes, etc., were found to be coexisting in $PLA_{212}-PEG_{44}$ THF/H_2O and $PLA_{212}-PEG_{44}$ dioxane/H_2O mixtures with 30 and 40 wt % water contents. Toroid micelles with new morphologies were also observed. These observations indicate that the vesicular micelles of amphiphilic block copolymers in mixed solvents fluctuate from time to time and are able to kinetically form different shapes of morphologies in the solutions. The membrane fluctuation of $PLA_{212}-PEG_{44}$ vesicles in mixed solvent was verified by dynamic light scattering.

Introduction

Polymer vesicles are closed spherical lamellar structures formed from amphiphilic block copolymers in selective solvents. Since the polymer vesicles are robust and have advanced mechanical properties over those of the vesicles formed from lipids and surfactants, they are considered to be promising candidates for use in the drug delivery and encapsulation.[1−3] Various synthetic amphiphilic block copolymers, like polystyrene-*b*-poly(acrylic acid) (PS−PAA),[3−8] polystyrene-*b*-poly(ethylene oxide) (PS−PEO),[9] poly(DL-lactide)-*b*-poly(ethylene glycol) (PLA−PEG),[2,10−12] polycaprolactone-*b*-poly(ethylene glycol) (PCL−PEG),[11,13] poly(ethylene oxide)-*b*-poly(propylene oxide)-*b*-poly(ethylene oxide) (PEO−PPO−PEO),[14] etc., have been reported to form vesicles in different conditions.[15−17] Efforts have been also dedicated to control the structure of polymer vesicles, such as size and wall thickness, by tuning the block length, block distribution, solvent properties and compositions, etc.[4,7,8]

The applications in biomedical fields require that the polymer vesicles should be biocompatible, nontoxic, and biodegradable. However, most synthetic amphiphilic block copolymers can only partially fulfill these strict requirements. Poly(lactide) (PLA) is a bio-based polymer with high biocompatibility. PLA is also biodegradable and can be degraded to regenerate lactide by thermal degradation or hydrolytic degradation.[18,19] Poly(ethylene glycol) (PEG) is hydrophilic and soluble in both water and organic solvents. PEG exhibits excellent biocompatibility, lack of toxicity, and absence of immunogenicity.[20] The combination of the characteristics of PLA and PEG is hence much attractive for biomedical and biotechnological applications. Copolymerization offered the possibility of such combination, and PLA−PEG diblock or triblock copolymers were then synthesized. Because of the biocompatible and biodegradable characteristics of the PLA−PEG block copolymers, the formation and applications of PLA−PEG or PLA−PEG−PLA micelles had thus been extensively investigated in the scopes of drug encapsulation, drug delivery, and drug-controlled release.[11,21−29] However, only a few studies reported on the vesicle formation of PLA−PEG and the systematical investigations of PLA−PEG vesicles are even fewer.[2,3,10−12]

In the present works, three narrow dispersed poly(DL-lactide)−poly(ethylene glycol) (PLA_x-PEG_{44}) diblock copolymers with fixed hydrophilic PEG block and various lengths of hydrophobic PLA block were synthesized via ring-opening polymerization. The micelle formation and micelle morphologies of the PLA_x-PEG_{44} diblock copolymers in selective solvents were investigated by using cryogenic transmission electron microscopy (cryo-TEM) as well as static and dynamic light scattering (SLS and DLS). The effects of hydrophobic block length on the micelle morphologies and sizes were discussed. Vesicular structures were found in PLA_x-PEG_{44} diblock copolymer with the longest PLA block length. The cryo-TEM results also indicate that the membranes of vesicular structures of PLA_x-PEG_{44} diblock copolymer in mixed solvents fluctuate from time to time and are able to kinetically form different shapes of morphologies at the same time in the solutions. The existence of membrane fluctuation was confirmed by DLS.

Experimental Section

Chemicals and Materials. DL-Lactide (LA, 3,6-dimethyl-1,4-dioxane-2,5-dione) and monomethoxy poly(ethylene glycol) with molecular weight of 2000 (M-PEG2000) were purchased from Acros, Inc. $AlEt_3$ was received from Aldrich. All other reagents were of analytical grade and commercially available.

Synthesis of Polylactide−Poly(ethylene glycol). The poly(DL-lactide)-*b*-poly(ethylene glycol) (PLA−PEG) diblock copolymers were synthesized via ring-opening polymerization of LA in the presence of M-PEG2000 according to a procedure described

*Corresponding author. E-mail: duby@zju.edu.cn.

Published on Web 10/14/2009

Table 1. Some Physical Parameters of the PLA_x-PEG_{44} Diblock Copolymers

samples	DL-LA (g)	conversion (%)	M_n[a] ($\times 10^{-3}$ g/mol)	M_n[b] ($\times 10^{-3}$ g/mol)	DP_{PLA}[b]	PDI[a]
$PLA_{56}-PEG_{44}$	1.5	86	7.7	6.0	56	1.06
$PLA_{134}-PEG_{44}$	2.0	65	12.0	11.6	134	1.08
$PLA_{212}-PEG_{44}$	3.0	77	23.4	17.2	212	1.14

[a] Determined by gel permeation chromatograph (GPC, calibrated with polystyrene standards). M_n is the number-average molecular weight, and PDI is the polydispersive index. [b] Calculated from ^{1}H NMR spectra of the diblock copolymers.

in detail elsewhere.[30] All involved chemicals and catalysts were treated and prepared accordingly. All operations were carried out under a dry Ar atmosphere with a Schlenk technique. Briefly, M-PEG2000 was dried by an azeotropic distillation with dry toluene. DL-Lactide was dried in vacuum for 2 h before use. The catalysts were prepared by adding a solution of $AlEt_3$ in toluene (1.0 M) into a solution of *N*-(2-hydroxybenzylidene)aniline in toluene under N_2 at room temperature, which were then heated to 75 °C and held for 2 h. The obtained catalysts were used without further purification. M-PEG2000 solution in toluene was added to the catalyst solution at room temperature. The mixture was heated to 75 °C and stirred for 2 h. Afterward, the mixture was cooled to room temperature, and the preset amount of LA solution in toluene was added. The mixture was then heated to 75 °C again, and the polymerization was allowed to continue for 24 h under magnetic stirring. The products were isolated by precipitation into hexane and filtered. The precipitates were dried in vacuum at room temperature until constant weight. The diblock copolymers were coded as PLA_x-PEG_{44}, in which the subscripts x and 44 are degrees of polymerization (DP) for PLA and M-PEG2000 blocks, respectively.

Preparation of PLA_x-PEG_{44} Micelle in Selective Solvents. The PLA_x-PEG_{44} diblock copolymers were first dissolved in tetrahydrofuran (THF) to obtain homogeneous solutions with preset concentrations of 0.45 wt %. To obtain micelle, distilled water was dropwisely (ca. 1 droplet per 10 s) added into the copolymer THF solutions under vigorous magnetic stirring. The addition of water was continued until the desired water content (20 wt %) was reached. The mixing solutions were then transferred to dialysis tubes with molecular cutoff of 3500 and dialyzed against distilled water for 3 days at room temperature in order to completely get rid of THF. The distilled water was frequently changed during the dialysis process. The obtained micelle aqueous solutions were transferred into clean volumetric glass flasks.

The $PLA_{212}-PEG_{44}$ micelles were also formed in THF/H_2O and dioxane/H_2O mixed solvents with various water content. Note that in these cases the initial polymer concentrations were 1, 0.45, and 0.2 wt %. A given amount of distilled water was dropwisely added into the copolymer solutions under vigorously magnetic stirring. The micelles formed in the THF/H_2O and dioxane/H_2O mixed solvents were directly subjected to further investigation without dialysis.

Instruments and Characterization. Number-average and weight-average molecular weights (M_n and M_w) and molecular weight distributions of PLA_x-PEG_{44} diblock copolymer were determined by gel permeation chromatograph (GPC, PL-GPC 220, Polymer Laboratories Ltd.) with tetrahydrofuran as the eluent and monodisperse polystyrene as the calibration standard. ^{1}H NMR of the copolymers was performed on a 300 MHz Varian Mercury Plus NMR instrument with $CDCl_3$ as solvent and tetramethylsilane (TMS) as internal standard.

The morphologies of the PLA_x-PEG_{44} micelles were observed with cryogenic transmission electron microscopy (cryo-TEM). The cryo-TEM measurements were carried out in the BioEM lab, State Key Lab of Biocontrol, School of life Sciences, Sun Yat-Sen University, Guangzhou 510275. For cryo-TEM, 4 μL of sample was applied to a holey carbon film grid (R1.2/1.3 Quantifoil Micro Tools GmbH, Jena, Germany), and then the excess solution was absorbed by filter paper from the other side of the grid. Afterward, the grid was immediately plunged into precooled liquid ethane for flash freeze at −172 °C. The cryo-grid was held in a Gatan 626 cryo-holder and transferred into TEM (JEOL JEM-2010 with 200 kV LaB_6 filament) at −172 °C. The micrographs were recorded by a Gatan 832 CCD camera at a magnification of 6000−50 000× and at the defocus of 3−5.46 μm.

The static and dynamic light scattering (SLS and DLS) of the micelle solutions were carried out on a Brookhaven Instrument BI-200SM with a laser wavelength of 636 nm at 25 °C. The micelle solutions used were the same as those for cryo-TEM imaging. Each micelle aqueous solution was diluted with distilled water to give a total liquid volume of 50 mL after the cryo-TEM measurements, while the micelle THF/H_2O solutions and dioxane/H_2O mixed solvents were used directly. The range of scattering angle θ used for SLS was from 40° to 150° with a step of 10°. DLS measurements were performed at five scattering angles between 60° and 120°, i.e., 60°, 75°, 90°, 105°, and 120°. The wave vector $q = (4\pi n/\lambda)\sin(\theta/2)$ with λ, n, and θ being the wavelength of the laser light in vacuum, the refractive index of solvent, and the scattering angle, respectively. The experimental data were analyzed with the help of software package supplied by the instrumental manufactory. The viscosities of THF/H_2O mixed solvents were measured by using a Ubbelohde viscometer at 25 °C, which are listed in Table S1 (see Supporting Information).

The membrane fluctuation of the $PLA_{212}-PEG_{44}$ vesicles in THF/H_2O mixed solvents was investigated by dynamic light scattering on a commercial spectrometer ALV/DLS/SLS-5022 at 25 °C. The range of scattering angles was from 15° to 150°. The samples were filtered through 0.45 μm PTFE filters before measurements. The data acquisition time was set to 5 min. The obtained time-average autocorrelation function was analyzed with the software package supplied by the manufacturer. These measurements were carried out in Hefei National Laboratory for Physical Sciences at Microscale, Department of Chemical Physics, University of Science and Technology of China.

Results and Discussion

Synthesis and Characterization of PLA_x-PEG_{44} Diblock Copolymers. Three PLA_x-PEG_{44} diblock copolymers with different molecular weights and compositions were obtained by varying the initial amount of LA and fixing other polymerization conditions. Figure S1 shows a typical ^{1}H NMR spectrum of a PLA−PEG diblock copolymer, which indicates the successful synthesis of the PLA−PEG diblock copolymer (see Supporting Information). The number-average molecular weights (M_n) of the PLA_x-PEG_{44} diblock copolymers can be then calculated from the ^{1}H NMR spectra. Figure S2 shows the GPC curves of the PLA−PEG diblock copolymers. It can be seen that all the block copolymers exhibited a narrow molecular weight distribution. Table 1 summarizes the preparation conditions and some physical parameters of the three PLA_x-PEG_{44} diblock copolymers.

PLA_x-PEG_{44} Micelles in Aqueous Solution. Figure 1 shows the cryo-TEM morphologies of PLA_x-PEG_{44} micelles in aqueous solutions. All of the micelle samples were prepared by first adding 20 wt % water into the initial copolymer THF solutions, which were then dialyzed against distilled water for 3 days. For $PLA_{56}-PEG_{44}$, branched and circular wormlike micelles were observed (Figure 1A).

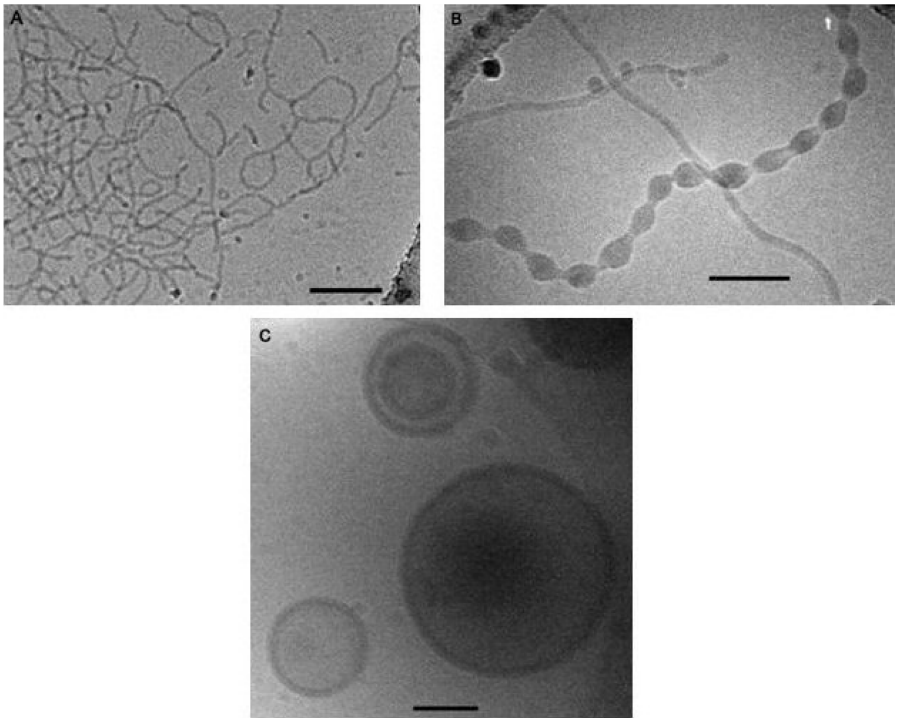

Figure 1. Cryo-TEM images of PLA_x-PEG_{44} micelles in aqueous solution. The concentrations of initial PLA_x-PEG_{44} THF solutions were 0.45 wt %. (A) $PLA_{56}-PEG_{44}$, (B) $PLA_{134}-PEG_{44}$, and (C) $PLA_{212}-PEG_{44}$. The scale bars in the images present 200 nm.

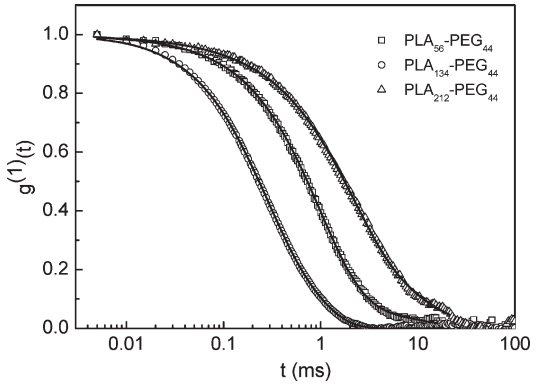

Figure 2. Electric-field autocorrelation function $g^{(1)}(t)$ of $PLA_{56}-PEG_{44}$, $PLA_{134}-PEG_{44}$, and $PLA_{212}-PEG_{44}$ micelles in aqueous solution measured at 25 °C and scattering angle of $\theta = 90°$. The solid lines are the best fits with eq 1 with fit quality of $R^2 = 0.999$.

The diameter of wormlike micelles was rather uniform and ca. 11 nm. With increasing the PLA block length to $x = 134$, mixed micelles with various morphologies including long tubes, small vesicles, necklace-like interconnected vesicles, and octopus-like open lamellae were coexisting in $PLA_{134}-PEG_{44}$ aqueous solution (Figure 1B and Figure S3 in Supporting Information). Further increasing the PLA block length to $x = 212$, only vesicular structures (including unilamellar vesicles and multilamellar vesicles) with large size distribution were observed (Figure 1C). The membrane thickness of the vesicles is uniform and ca. 31 nm regardless of the size and structure of vesicles.

Considering the effect of hydrophobic block length on the micelle morphologies of amphiphilic diblock copolymers, a general view is that with increasing the length of hydrophobic block the micelle morphology tends to transform from sphere via rod- or wormlike micelles to bilayer structures or vesicles, for example PS−PAA, PS−PEO, P4VP−PS−P4VP, polybutadiene-*b*-poly(2-vinylpyridine) (PB−P2VP), etc.[9,15,31−35] However, a different tendency seems to be found for PLA−PEG diblock copolymers. With increasing the hydrophilic PEG fractions (f_{EO}) of the diblock copolymers, the morphology of PLA−PEG micelles shifts from spherical micelles ($f_{EO} < 20\%$) to vesicles ($f_{EO} \sim 20-42\%$) or wormlike micelles ($f_{EO} > 42\%$),[11] whereas Meng et al.[10] and Lee et al.[12] reported on the vesicle formation of PEG−PDLLA diblock copolymers with relative longer PDLLA block length in aqueous solution. The cryo-TEM results shown in Figure 1 indicate that the micelle morphology transforms from wormlike micelle via open lamellae into closed lamellae (vesicles) when increasing length of hydrophobic PLA blocks from $x = 56$ to $x = 212$ for PLA_x-PEG_{44} diblock copolymers. These results are consistent with the general view found in many other diblock copolymers.[9,15,31−35] The formation of micelles, size, and morphology of micelles as well as their evolution partway of coil−coil diblock copolymers in selective solvents are mainly dependent on the energy balance among the stretching of the core-forming block, the interfacial tension between the core and the solvent outside the core region, and the repulsion among the corona chains.[31,32,36−38] With increasing the hydrophobic PLA block length, the degree of stretching of PLA block decreases. Furthermore, the degree of stretching of PLA block also decreases when the micelle structures change from wormlike to vesicular. The area per corona chain (PEO) on the core (PLA) surface will decrease as the micelle structures transform from wormlike to vesicular, which decreases the interfacial energy between the PLA core and surrounding water. As a consequence, the micelles of PLA_x-PEG_{44} in aqueous solution transform from wormlike micelles for $PLA_{56}-PEG_{44}$ into vesicular structures for $PLA_{212}-PEG_{44}$ in order to minimize the overall free energy of the system (cf. Figure 1).

The overall structures of PLA_x-PEG_{44} micelles in aqueous solution were then investigated with DLS and SLS.

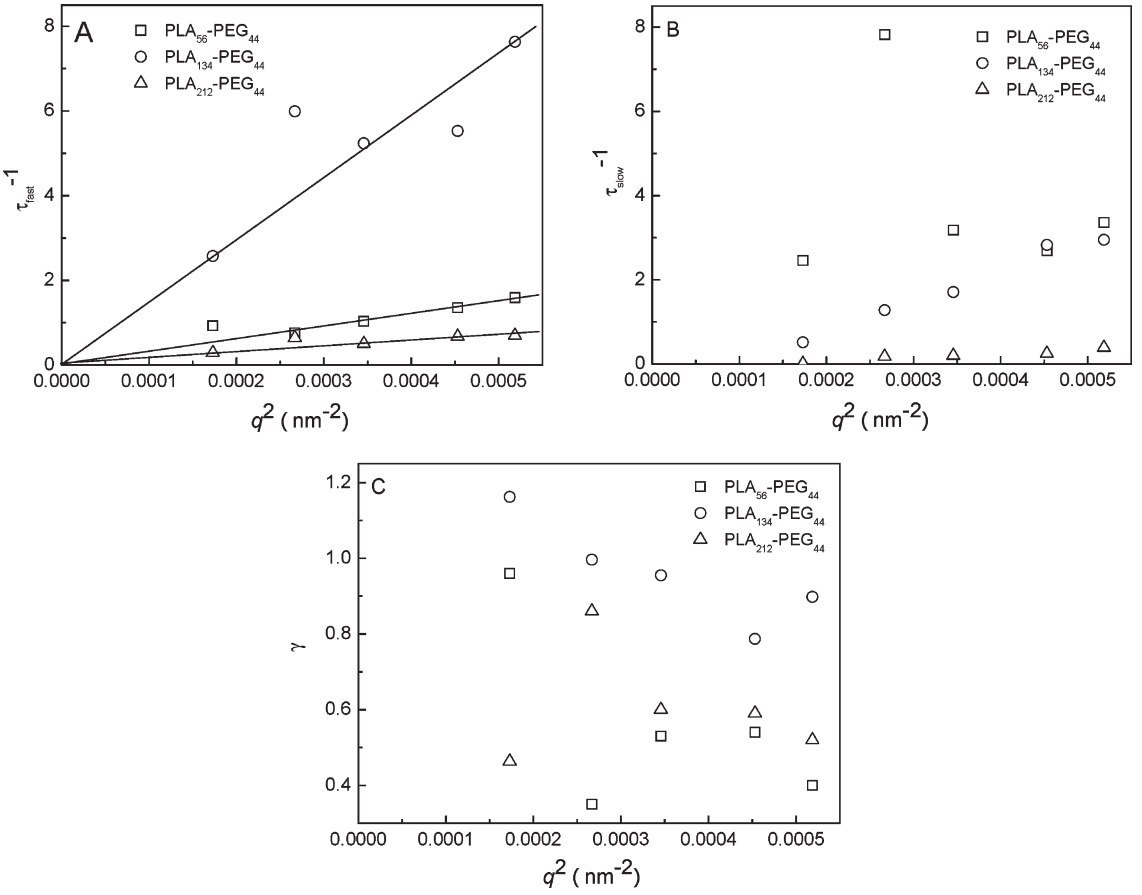

Figure 3. Values of τ_{fast} (A), τ_{slow} (B), and γ (c) as a function of square of wave vector q^2. The solid lines in (A) are the guide to the eyes.

The DLS data were found to be strongly dependent on the wave vector q or scattering angle θ, which indicate the large polydispersity of the micelles or the existence of elongated micelles.[39] The electric-field autocorrelation function $g^{(1)}(t)$ of PLA_x-PEG_{44} micelles in aqueous solutions cannot be fitted with the simple cumulant fit method.[40,41] Figure 2 shows the electric-field autocorrelation function $g^{(1)}(t)$ of PLA_x-PEG_{44} micelles in aqueous solutions obtained at 25 °C and $\theta = 90°$.[42] It can be clearly seen that there is slow relaxation mode at long relaxation times. Wormlike (or long rod) micelles can entangle with each other in the solution.[43,44] The slow relaxation mode may be then associated with the disentanglement relaxation of the wormlike micelles or the relaxation of large micelles. A stretched exponential function is used to describe the slow relaxation mode. The electric-field autocorrelation function is then fitted with eq 1:[45]

$$g^{(1)}(t) = A_{fast}\exp\left(-\frac{t}{\tau_{fast}}\right) + A_{slow}\exp\left[-\left(\frac{t}{\tau_{slow}}\right)^{\gamma}\right] \quad (1)$$

where the fast mode τ_{fast} reflects the collective diffusion of the micelles, the slow mode τ_{slow} presents the effective slow relaxation time, and the stretched exponent γ ($0 < \gamma \leq 1$) is inversely proportional to the width of the distribution of relaxation time. A low value of γ indicates a large width of the distribution of relaxation times.[45] The prefactors A_{fast} and A_{slow} are the amplitudes of the fast and slow relaxation modes, respectively, and the sum $A_{fast} + A_{slow}$ is close to 1. The solid lines in Figure 2 show that the electric-field autocorrelation function $g^{(1)}(t)$ of PLA_x-PEG_{44} micelles in aqueous solutions can be well described by eq 1 (fit quality of $R^2 = 0.999$).

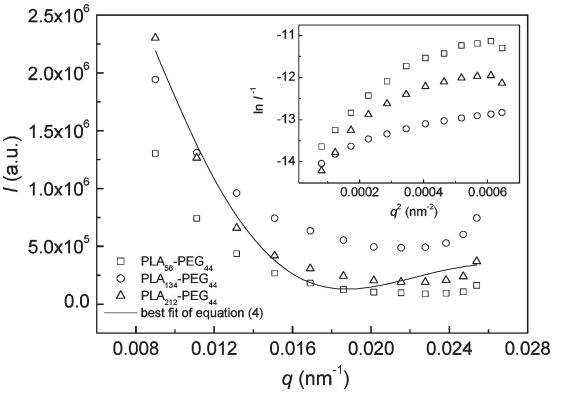

Figure 4. Static light scattering intensity of $PLA_{56}-PEG_{44}$, $PLA_{134}-PEG_{44}$, and $PLA_{212}-PEG_{44}$ micelles in aqueous solution measured at 25 °C as a function of wave vector, q. The solid line is the best fit of eq 4 to $PLA_{212}-PEG_{44}$ data set with fit quality of $R^2 = 0.98$. The inset is the corresponding Guinier plots, and no linear dependence can be found.

Figure 3 shows the values of τ_{fast}, τ_{slow}, and γ as a function of square of wave vector q^2. It can be seen that the relation of $1/\tau_{fast} \sim q^2$ basically holds (Figure 3A), indicating that the nature of collective diffusion for the fast mode, whereas the relation of $1/\tau_{slow} \sim q^2$ does not hold for the slow relaxation mode (Figure 3B). The values of γ vary with the wave vector (or scattering angle) and indicate the wide distribution of relaxation times. For semiquantitative comparison, the apparent hydrodynamic radius R_h of the PLA_x-PEG_{44} micelles in aqueous solution can be roughly estimated from the fast relaxation mode,

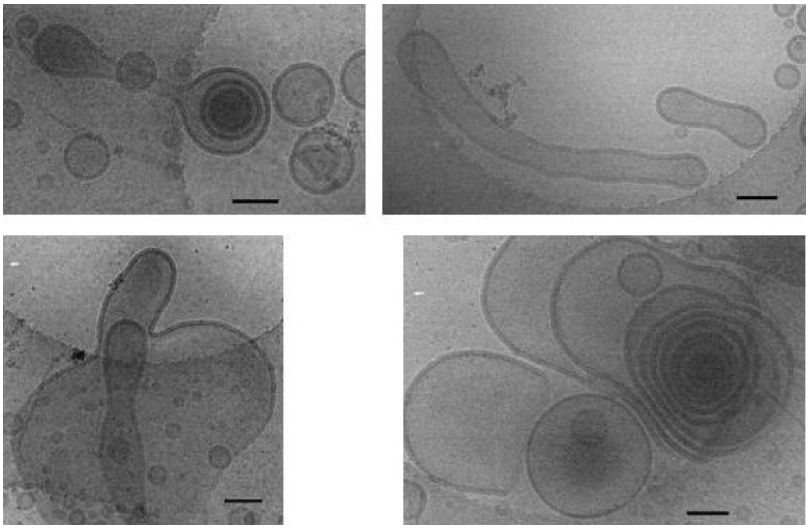

Figure 5. Cryo-TEM vesicle morphologies of PLA_{212}−PEG_{44} in THF/H_2O mixture with 30 wt % contents of water. The initial concentration of PLA_{212}−PEG_{44} THF solutions was 1 wt %. The scale bars in the images present 200 nm.

τ_{fast} at scattering angle $\theta = 90°$ by using Stokes−Einstein equation given as

$$R_h = \frac{k_B T}{6\pi\eta}(\tau_{fast} q^2) \quad (2)$$

where $k_B = 1.4 \times 10^{-23}$ J K^{-1} is the Boltzmann constant, $T = 298.15$ K is the absolute temperature, and $\eta = 0.89 \times 10^{-3}$ N m^{-2} s is the viscosity of water at 25 °C. The apparent R_h is then calculated to be ~84, ~19, and ~ 171 nm for PLA_{56}−PEG_{44}, PLA_{134}−PEG_{44}, and PLA_{212}−PEG_{44} micelles in aqueous solutions, respectively. These results are consistent with the micelle sizes in cryo-TEM images (cf. Figure 1).

Figure 4 shows the intensity of static light scattering as a function of wave vector, q. It can be seen that the angular distributions of the scattered light strongly anisotropic, indicating the existence of large aggregates in the solutions.[46] For small aggregates with $qR_g < 1$, where R_g is the radius of gyration of the aggregate, the SLS data can be described by the so-called Guinier plot:[47,48]

$$\left(\frac{KC}{R_{vv}(q)}\right)_{c\to 0} \approx \frac{1}{M_w} \exp\left(\frac{1}{3}\langle R_g^2\rangle_z q^2\right) \quad (q\langle R_g^2\rangle^{1/2} < 1) \quad (3)$$

where $K = 4\pi^2 n^2 (dn/dC)^2/(N_A\lambda^4)$ with dn/dC, N_A, λ, and n being the specific refractive index increment of the solution, the Avogadro number, the wavelength of the laser light in vacuum (here $\lambda = 636$ nm), and the refractive index of solvent, respectively. R_w is the Rayleigh ratio, corresponding to the scattering intensity, I. M_w is the molecular weight of the micelle. Here, $qR_g > 1$ for the wormlike micelles and vesicles of PLA_x−PEG_{44} in aqueous solutions; eq 3 cannot be used to describe the SLS data (inset of Figure 4). However, Ristori et al. showed that the vesicular structures in solution can be described with a form factor of $P(q) = \sin^2(qR)/(qR)^2$, and the SLS data curve can be fitted with[46]

$$I(q) = A\frac{\sin^2(qR)}{(qR)^2} + B \quad (4)$$

where R is the mean radius of vesicles with a membrane thickness δ ($\delta \ll R$ and $q\delta \ll 1$). The solid line in Figure 4 is the best fit of eq 4 to the data set of PLA_{212}−PEG_{44} micelles in aqueous solution (fit quality of $R^2 = 0.98$). The obtained mean radius of $R = 167$ nm, which is close to $R_h \sim 171$ nm estimated from eqs 1 and 2. It is known that the microstructure of the objects in solution can be characterized by the ratio of $\langle R_g\rangle/\langle R_h\rangle$. For linear and flexible polymer chains in good solvent, $\langle R_g\rangle/\langle R_h\rangle$ is around 1.5, while for uniform hard spheres, $\langle R_g\rangle/\langle R_h\rangle$ is 0.778. The $\langle R_g\rangle/\langle R_h\rangle$ ratio of hollow sphere is theoretically expected to be 1. The results of $R/R_h \sim 0.977$ clearly evident the vesicular structures of PLA_{212}−PEG_{44} micelles in aqueous solution, which is in excellent agreement with the cryo-TEM image (cf. Figure 1C).

The results of light scattering measurements are consistent with the cryo-TEM results, which clearly show the existence of long micelles in PLA_{56}−PEG_{44} and PLA_{134}−PEG_{44} aqueous solutions and the large size distribution of vesicles in PLA_{212}−PEG_{44} aqueous solution.

Vesicular Structures of PLA_{212}−PEG_{44} Micelles in THF/H_2O and Dioxane/H_2O Mixed Solvents. The polymeric vesicle can encapsulate more drugs so that they are considered to have important applications in drug-delivery system. Here, we focused on the vesicle-forming PLA_{212}−PEG_{44} block copolymer. The effect of solvent composition on the vesicle morphology of PLA_{212}−PEG_{44} was then investigated. A predesired amount of distilled water (30 and 40 wt %) was dropwisely added into PLA_{212}−PEG_{44} THF solution and PLA_{212}−PEG_{44} dioxane solution with initial concentration of 1 wt % under vigorously magnetic stirring. The micelles formed in the THF/H_2O and dioxane/H_2O mixing solutions were then directly subjected to cryo-TEM and DLS studies without dialysis. Interestingly, various vesicular structures with different shapes are found to be coexisting in the mixed solutions (Figures 5−8 and Supporting Information). Figure 5 shows the selected vesicular structures observed in PLA_{212}−PEG_{44} THF/H_2O solution with 30 wt % water content. Large polydisperse vesicles, entrapped vesicles, hollow concentric vesicles, and ellipsoidal vesicles as well as open bending lamellae are coexisting. Vesicular structures with special shapes are also found (lower-left image of Figure 5). Figure 6 shows the selected vesicular structures observed in PLA_{212}−PEG_{44} THF/H_2O solution with 40 wt % water content. Again, vesicular structures with various shapes coexist. Large vesicles with possible tubes in the wall are found. PLA_{212}−PEG_{44} forms

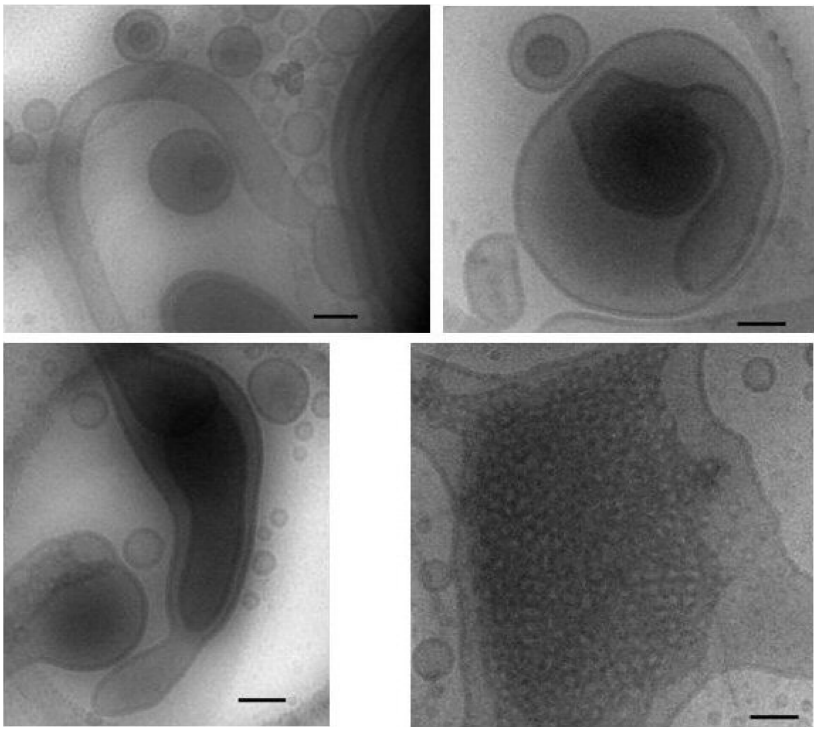

Figure 6. Cryo-TEM vesicle morphologies of PLA_{212}−PEG_{44} in THF/H_2O mixture with 40 wt % contents of water. The initial concentration of PLA_{212}−PEG_{44} THF solutions was 1 wt %. The scale bars in the images present 200 nm.

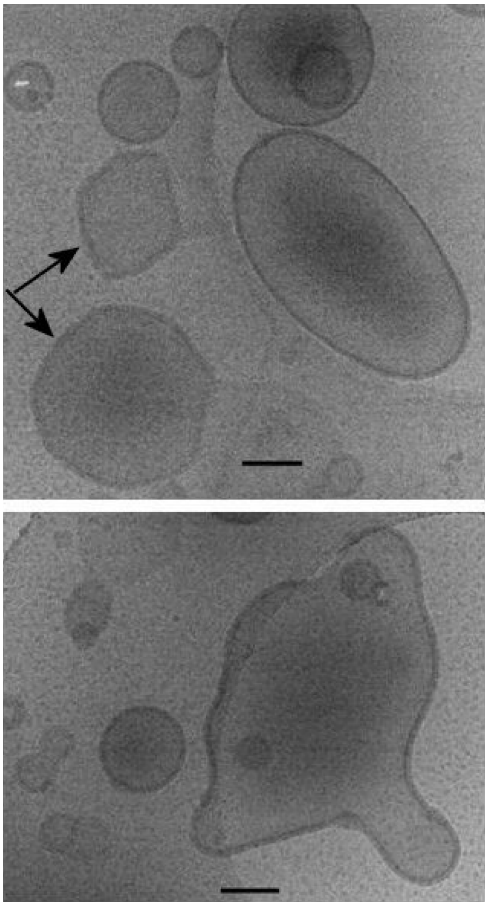

Figure 7. Cryo-TEM vesicle morphologies of PLA_{212}−PEG_{44} in dioxane/H_2O mixture with 40 wt % contents of water. The initial concentration of PLA_{212}−PEG_{44} dioxane solutions was 1 wt %. The scale bars in the images present 200 nm.

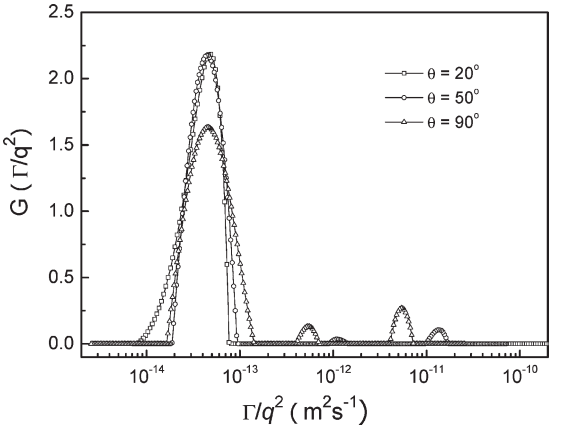

Figure 8. Angular dependence of q^2-normalized line-width distribution ($G(\Gamma/q^2)$ of the PLA_{212}−PEG_{44} vesicles in THF/H_2O mixture with 40 wt % contents of water. The initial concentration of PLA_{212}−PEG_{44} THF solutions was 1 wt %.

vesicles in dioxane/H_2O mixed solvent with 40 wt % water content as well. Figure 7 shows typical PLA_{212}−PEG_{44} vesicles with irregular shapes in dioxane/H_2O mixed solvent with 40 wt % water content. A fishlike vesicle with two entrapped small vesicles as eyes is observed (lower-right image of Figure 7).

The multiple vesicular morphologies from block copolymers in solution have been classified by Burke et al.[49] Six different vesicular morphologies are summarized. They are uniform bilayer vesicles, large polydisperse bilayer vesicles, entrapped vesicles, onions, hollow concentric vesicles, and vesicles with hollow tubes in the wall. The last two vesicular morphologies are rarely observed. In the literature, it was only found in a solution of 10 wt % PS_{132}−PAA_{20} in dioxane/H_2O mixed solvent with 25 wt % water content following a dialysis procedure.[49] Vesicles with hollow tubes

in the wall were observed in PS−PEO diblock copolymer systems.[50] Figures 5 and 6 show that such nonclassical vesicular morphologies coexist in PLA_{212}−PEG_{44} THF/H_2O mixing solution with 30 and 40 wt % water contents. It was thought that the existing of intermediate micelle structures is related to the lower mobility of the polymer chains,[51] the lower kinetics of morphological transitions, and possibly the boundary crossing between different regions of stability during the water addition and dialysis procedures.[50]

Vesicles of flexible bilayers are expected to undergo shape fluctuation. The amplitude and frequency of such fluctuation are dependent on the bilayer rigidity. Ellipsoidal shape modes of vesicular fluctuation was theoretically expected.[52] The thermal fluctuations of single component phospholipid vesicles have been also observed by dynamic light scattering with a laser emitting in the ultraviolet.[53] Furthermore, the fission and fusion of vesicles are rare observed because the ripening and coarsening of vesicles can be very slow. Hence, the metastable intermediate states may be even trapped in the system.[3,54] The cryo-TEM images indicate that the vesicular structures of PLA_{212}−PEG_{44} in THF/H_2O and dioxane/H_2O mixtures were in dynamic and kinetic equilibrium states. The shapes of the vesicular structures of PLA_{212}−PEG_{44} frequently fluctuate as a course of time. Fission, fusion, fluctuation, and shape rearrangement of the vesicles may happen in the mixtures, which result in the coexistence of various nonclassical vesicles together with classical spherical vesicles. During the sample preparation for cryo-TEM experiments, such fluctuated vesicular structures of PLA_{212}−PEG_{44} with different shapes in mixed solvents were suddenly frozen by cold liquid ethane and were confirmed by cryo-TEM (cf. Figures 5, 6, and 7). Especially, the irregular shapes were strong evidence that the membrane of the vesicles fluctuate in the solution (arrows in Figure 7).

As was mentioned above, the thermal fluctuation of vesicles has been theoretically expected and experimentally observed in single component phospholipid vesicles by dynamic light scattering.[52,53] In an investigation of porous cross-linked polystyrene hollow spheres by dynamic light scattering, Wang and Wu[55] had found that the slowest observable vibration of such porous spherical shell immersed in liquid involves only a portion of the shell, which was hence corresponding to the fluctuation of the shell. Their results further indicated that the shell fluctuation of polymeric hollow spheres can be observed by dynamic light scattering at larger scattering angle. Accordingly, if the membrane fluctuation of the PLA_{212}−PEG_{44} vesicles in mixed solvents shown above by cryo-TEM images was real, it should be also observed by dynamic light scattering.

To testify such speculation, PLA_{212}−PEG_{44} vesicles in THF/H_2O mixed solvent with 40 wt % water contents were chosen for further investigation by dynamic light scattering. Three different initial concentrations of PLA_{212}−PEG_{44} THF solutions were studied, i.e., 1, 0.45, and 0.2 wt %. According to Wang and Wu's report,[55] only the translational diffusion of the vesicles will be observed at smaller scattering angle with $\langle R_g \rangle q < 1$, whereas the membrane fluctuation starts to contribute to the time-average autocorrelation function for $\langle R_g \rangle q > 1$. By applying the analysis method proposed by them,[55] the angular dependence of q^2-normalized line-width distribution ($G(\Gamma/q^2)$ of the PLA_{212}−PEG_{44} vesicles in THF/H_2O mixture with 40 wt % contents of water is shown in Figure 8. Clearly, a single distributed peak was observed when scattering angle $\theta = 20°$. By taking the average hydrodynamic radius of PLA_{212}−PEG_{44} vesicles, $R_h \sim 420$ nm as the value of R_g, $\langle R_g \rangle q$ was estimated to be ~2 for $\theta = 20°$. Additional second and third small peaks appeared with further increasing scattering angle. Typical data curves obtained at $\theta = 50°$ and $\theta = 90°$ are shown in Figure 8. It can be seen that the first peak was almost independent of scattering angle, corresponding to the translational diffusion of vesicles. The third peak was attributed to the slowest observable vibration of the vesicles, i.e., $\langle \Gamma_{slowest} \rangle$. The slowest vibration mode appeared at large $\langle R_g \rangle q$ value only involved a portion of vesicle, indicating the existence of the membrane fluctuation of vesicles, which was consistent with those observed in porous cross-linked polystyrene hollow spheres.[55] The appearance of the second peak may be possibly due to the polydispersity of the vesicle shapes (cf. Figure 6). The average line width $\langle \Gamma_{slowest} \rangle$ of the slowest observable vibration of the hollow sphere has been confirmed to be proportional to the scattering wave vector q, i.e., $\langle \Gamma_{slowest} \rangle \propto q$.[55] Such a linear relation of $\langle \Gamma_{slowest} \rangle \propto q$ was also found here for PLA_{212}−PEG_{44} vesicles in THF/H_2O mixed solvent prepared from various initial concentrations, as shown in Figure 9. Figure 9 also suggests that the initial concentrations of PLA_{212}−PEG_{44} in THF had not significant effects on the formation of vesicular structures in THF/H_2O mixed solvents. The values of $\langle \Gamma_{slowest} \rangle$ of PLA_{212}−PEG_{44} vesicles were in the similar order of magnitude with those found in porous cross-linked polystyrene hollow spheres.[55] These DLS results not only verified the existence of membrane fluctuation of PLA_{212}−PEG_{44} vesicles in mixed solvents but also indicated that the membranes of PLA_{212}−PEG_{44} vesicles were sufficiently soft, leading to the observation of slowest vibration mode.[52]

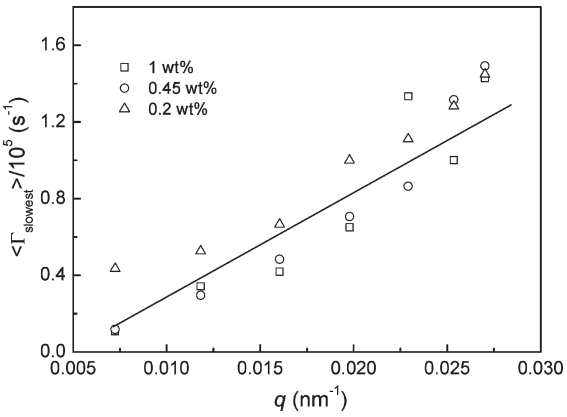

Figure 9. Scattering vector dependence of the average line width $\langle \Gamma_{slowest} \rangle$ of the slowest observable vibration of the PLA_{212}−PEG_{44} vesicles in THF/H_2O mixture with 40 wt % contents of water. The initial concentrations of PLA_{212}−PEG_{44} THF solutions were 1, 0.45, and 0.2 wt %. The line is the guide for the eye.

Conclusion

In summary, the micelle behavior of three diblock copolymers, PLA_{56}−PEG_{44}, PLA_{134}−PEG_{44}, and PLA_{212}−PEG_{44}, in selective solvents was investigated by cryo-TEM, SLS, and DLS. It was found that the micelles of PLA_x−PEG_{44} in aqueous solution transform from wormlike micelles for PLA_{56}−PEG_{44} into vesicular structures for PLA_{212}−PEG_{44} with increasing the length of hydrophobic PLA block. Various vesicular morphologies, such as entrapped vesicles, hollow concentric vesicles, ellipsoidal vesicles, open bending lamellae, etc., were found to coexist for PLA_{212}−PEG_{44} in THF/H_2O and dioxane/H_2O mixed solvents with 30 and 40 wt % water contents. These results suggest that the vesicular structures of PLA_{212}−PEG_{44} in mixed solvents fluctuate frequently and are able to kinetically form various shapes of morphologies in the solutions. The membrane fluctuation of PLA_{212}−PEG_{44} vesicles in THF/H_2O mixed solvents were confirmed by dynamic light scattering measurements.

Acknowledgment. We thank the National Natural Science Foundation of China (20604022, 20874087), Scientific Research Foundation for Returned Overseas Chinese Scholars (Ministry of Education), and the Zhejiang Provincial Natural Science Foundation of China (Y406029) for financial support. We thank Prof. Guangzhao Zhang and Dr. Yi Hou in University of Science and Technology of China for the help in the DLS measurements of membrane fluctuation and fruitful discussions. We thank Prof. Qiang Zheng and Dr. Yonggang Shangguan for the use of BI-200SM. We also thank the editor and unknown reviewers for their useful and constructive comments and suggestions.

Supporting Information Available: Experimental details. This material is available free of charge via the Internet at http://pubs.acs.org.

References and Notes

(1) Antonietti, M.; Forster, S. *Adv. Mater.* **2003**, *15*, 1323.
(2) Discher, B. M.; Won, Y. Y.; Ege, D. S.; Lee, J. C. M.; Bates, F. S.; Discher, D. E.; Hammer, D. A. *Science* **1999**, *284*, 1143.
(3) Discher, D. E.; Eisenberg, A. *Science* **2002**, *297*, 967.
(4) Luo, L. B.; Eisenberg, A. *Langmuir* **2001**, *17*, 6804.
(5) Luo, L. B.; Eisenberg, A. *J. Am. Chem. Soc.* **2001**, *123*, 1012.
(6) Shen, H. W.; Eisenberg, A. *J. Phys. Chem. B* **1999**, *103*, 9473.
(7) Azzam, T.; Eisenberg, A. *Angew. Chem., Int. Ed.* **2006**, *45*, 7443.
(8) Choucair, A.; Lavigueur, C.; Eisenberg, A. *Langmuir* **2004**, *20*, 3894.
(9) Zhang, L. F.; Eisenberg, A. *Polym. Adv. Technol.* **1998**, *9*, 677.
(10) Meng, F. H.; Hiemstra, C.; Engbers, G. H. M.; Feijen, J. *Macromolecules* **2003**, *36*, 3004.
(11) Ahmed, F.; Discher, D. E. *J. Controlled Release* **2004**, *96*, 37.
(12) Lee, Y.; Chang, J. B.; Kim, H. K.; Park, T. G. *Macromol. Res.* **2006**, *14*, 359.
(13) Wittemann, A.; Azzam, T.; Eisenberg, A. *Langmuir* **2007**, *23*, 2224.
(14) Bryskhe, K.; Jansson, J.; Topgaard, D.; Schillen, K.; Olsson, U. *J. Phys. Chem. B* **2004**, *108*, 9710.
(15) Walther, A.; Goldmann, A. S.; Yelamanchili, R. S.; Drechsler, M.; Schmalz, H.; Eisenberg, A.; Muller, A. H. E. *Macromolecules* **2008**, *41*, 3254.
(16) Rank, A.; Hauschild, S.; Forster, S.; Schubert, R. *Langmuir* **2009**, *25*, 1337.
(17) Kickelbick, G.; Bauer, J.; Huesing, N.; Andersson, M.; Holmberg, K. *Langmuir* **2003**, *19*, 10073.
(18) Hubbell, J. A. *Bio/Technology* **1995**, *13*, 565.
(19) Anderson, J. M.; Shive, M. S. *Adv. Drug Delivery Rev.* **1997**, *28*, 5.
(20) Yamaoka, T.; Tabata, Y.; Ikada, Y. *J. Pharm. Sci.* **1994**, *83*, 601.
(21) Jeong, B.; Bae, Y. H.; Lee, D. S.; Kim, S. W. *Nature* **1997**, *388*, 860.
(22) Yasugi, K.; Nagasaki, Y.; Kato, M.; Kataoka, K. *J. Controlled Release* **1999**, *62*, 89.
(23) Hagan, S. A.; Coombes, A. G. A.; Garnett, M. C.; Dunn, S. E.; Davis, M. C.; Illum, L.; Davis, S. S.; Harding, S. E.; Purkiss, S.; Gellert, P. R. *Langmuir* **1996**, *12*, 2153.
(24) Yamamoto, Y.; Yasugi, K.; Harada, A.; Nagasaki, Y.; Kataoka, K. *J. Controlled Release* **2002**, *82*, 359.
(25) Yoo, H. S.; Park, T. G. *J. Controlled Release* **2001**, *70*, 63.
(26) Jeong, J. H.; Lim, D. W.; Han, D. K.; Park, T. G. *Colloids Surf., B* **2000**, *18*, 371.
(27) Li, X. R.; Yuan, X. Y. *Prog. Chem.* **2007**, *19*, 973.
(28) He, G. S.; Ma, L. L.; Pan, J.; Venkatraman, S. *Int. J. Pharm.* **2007**, *334*, 48.
(29) Riley, T.; Heald, C. R.; Stolnik, S.; Garnett, M. C.; Illum, L.; Davis, S. S.; King, S. M.; Heenan, R. K.; Purkiss, S. C.; Barlow, R. J.; Gellert, P. R.; Washington, C. *Langmuir* **2003**, *19*, 8428.
(30) Du, Z. X.; Xu, J. T.; Yang, Y.; Fan, Z. Q. *J. Appl. Polym. Sci.* **2007**, *105*, 771.
(31) Zhang, L. F.; Eisenberg, A. *J. Am. Chem. Soc.* **1996**, *118*, 3168.
(32) Zhang, L. F.; Eisenberg, A. *Science* **1995**, *268*, 1728.
(33) Tung, P. H.; Kuo, S. W.; Chen, S. C.; Lin, C. L.; Chang, F. C. *Polymer* **2007**, *48*, 3192.
(34) Won, Y. Y.; Davis, H. T.; Bates, F. S. *Science* **1999**, *283*, 960.
(35) Yu, Y.; Zhang, L.; Eisenberg, A. *Macromolecules* **1998**, *31*, 1144.
(36) Zhang, L.; Yu, K.; Eisenberg, A. *Science* **1996**, *272*, 1777.
(37) Yu, Y. S.; Eisenberg, A. *J. Am. Chem. Soc.* **1997**, *119*, 8383.
(38) Choucair, A.; Eisenberg, A. *Eur. Phys. J. E* **2003**, *10*, 37.
(39) Scarzello, M.; Klijn, J. E.; Wagenaar, A.; Stuart, M. C. A.; Hulst, R.; Engberts, J. *Langmuir* **2006**, *22*, 2558.
(40) Zhang, L. F.; Barlow, R. J.; Eisenberg, A. *Macromolecules* **1995**, *28*, 6055.
(41) He, Y. Y.; Li, Z. B.; Simone, P.; Lodge, T. P. *J. Am. Chem. Soc.* **2006**, *128*, 2745.
(42) Nie, J.; Du, B.; Oppermann, W. *J. Phys. Chem. B* **2006**, *110*, 11167.
(43) Nystrom, B.; Thuresson, K.; Lindman, B. *Langmuir* **1995**, *11*, 1994.
(44) Sun, Z.; Wang, C. H. *Macromolecules* **1994**, *27*, 5667.
(45) Ngai, K. L. *Adv. Colloid Interface Sci.* **1996**, *64*, 1.
(46) Ristori, S.; Appell, J.; Porte, G. *Langmuir* **1996**, *12*, 686.
(47) Michael, R.; Ralph, H. C. *Polymer Physics*; Oxford University Press: New York, 2003; p 85.
(48) Zimm, B. H. *J. Chem. Phys.* **1948**, *16*, 1009.
(49) Burke, S.; Shen, H. W.; Eisenberg, A. *Macromol. Symp.* **2001**, *175*, 273.
(50) Yu, K.; Bartels, C.; Eisenberg, A. *Langmuir* **1999**, *15*, 7157.
(51) Yu, K.; Eisenberg, A. *Macromolecules* **1998**, *31*, 3509.
(52) Milner, S. T.; Safran, S. A. *Phys. Rev. A* **1987**, *36*, 4371.
(53) Brocca, P.; Cantu, L.; Corti, M.; Del Favero, E. *Trends Colloid Interface Sci.* **2000**, *115*, 181.
(54) Olsson, U.; Wennerstrom, H. *J. Phys. Chem. B* **2002**, *106*, 5135.
(55) Wang, C. Q.; Wu, C. *Macromolecules* **2003**, *36*, 9285.